كلية الهندسة بشبرا
FACULTY OF ENGINEERING AT SHOUBRA
ERJ
PRINT ISSN 3009-6049
ONLINE ISSN 3009-6022

**ENGINEERING RESEARCH JOURNAL (ERJ)**
Volume (54),Issue (1)
January 2025, pp:23-34
https://erjsh.journals.ekb.eg

# Enhancing Concrete Prism Strength Using External Confining Pressure

**Ahmed. I. EL Dosoky [1,*], Hossameldin hamad hassan [1], Abeer M Erfan [1], A El-Sayed Taha [1], Tamer Elafandy [2]**

[1] *Civil Engineering Department, Faculty of Engineering at Shoubra, Benha University, Cairo, Egypt.*
[2] *Reinforced concrete Department, National Center for Building Research*
**Corresponding author*
*E-mail address: eldsokyahmed926@gmail.com, hossameldin.hamad@feng.bu.edu.eg.com, abir.arfan@feng.bu.edu.eg, taha.ibrahim@feng.bu.edu.eg, tamer_elafandy@yahoo.com*

**Abstract:** The primary objective of this research endeavor is to examine the influence of applying active external confining pressure along the longitudinal axis of prisms, utilizing a series of elongated members secured in place by multiple steel strips. This investigation delves into the behavioral characteristics and failure loads of these strengthened prisms through a comprehensive experimental program involving thirteen specimens. The empirical results unequivocally demonstrate a substantial enhancement in the ductility and strength of concrete prisms when subjected to external confining pressure. Notably, the effectiveness of external confinement was observed to be more pronounced in ordinary concrete (Fcu=20 N/mm$^2$), compared to high-strength concrete (Fcu=40:50 N/mm$^2$). Furthermore, at a certain amount of external pressure , the effect of increasing pressure on the strength of concrete prims started to diminish. The experimental test results were rigorously validated through the utilization of the ABAQUS finite element software. The finite element models generated in this study exhibited commendable agreement with experimental outcomes. Moreover, an equation has been proposed for the design of concrete prisms subjected to external confining pressure, demonstrating its predictive accuracy in estimating the ultimate load capacity.

**Keywords:** column ,strengthening ,steel jacket.

## 1. Introduction

When concrete is subjected to uniaxial compression, Poisson's effect gives rise to transverse strains that manifest as radial expansion. This volumetric expansion can be effectively mitigated through the application of lateral confinement techniques. By restricting the transverse expansion of concrete, these techniques induce a triaxial state of stress, thereby enhancing both the strength and ductility of the material. A significant deficiency often encountered in older concrete columns is the lack of lateral confinement. As weaker concrete structural members, columns restrained by ties or spirals are particularly susceptible to Poisson's effect, leading to lateral expansion. To counteract this and improve ductility and strength, it is imperative to increase the extent and coverage of lateral steel by encircling the concrete.

The technique of strengthening concrete columns with steel jackets offers several distinct advantages over alternative methods. Notably, it results in a negligible increase in weight and a minimal expansion of the column's cross-section. Moreover, this technique enhances the ductility and stiffness of the original column while significantly augmenting its shear strength, particularly when subjected to lateral loads. Priestley [1] has proposed a design equation for calculating the requisite thickness of steel jackets necessary to enhance the shear strength of both circular and rectangular columns. Lisantono et al. [2] have conducted extensive research on the application of steel jackets to strengthen reinforced concrete columns. Their investigations have contributed significantly to the understanding and refinement of this technique.

One of the most prominent techniques in which active confinement happens before the applied column stresses reach the axial compressive strength is by applying external confining which prevents lateral strains and volume increasing. The effect of confining pressure is to induce a tri-axial state of stress in the concrete which exhibits superior behavior in both strength and ductility more than concrete under uniaxial compression. Pressurized Steel Jacket technique was suggested by EL Tuhami [3]. It is the same as the ordinary steel jacket except that horizontal steel plates were welded under external pressure applied in corner steel angles. Active confinement leads to an increase in column ductility, durability, stiffness, ultimate compressive capacity, and shear resistance and improves column durability.

EL Tuhami [4] illustrated that the increase of applied confining pressure produces higher ultimate capacity and ductility. Besides that, he found that the increase in the number of steel pattern plates increases the ultimate load capacity and ductility.

EL Tuhami [5] demonstrated that the behavior of the tested specimens including the load-deflection relationship, failure modes, and ultimate capacity of the columns indicates better performance of the strengthened specimens.

EL Tuhami [6] confirmed that the reliability and efficiency of the suggested column-strengthening technique. In addition, the proposed technique overcomes the difficulties that may arise when retrofitting RC columns with inaccessible faces and columns with large length-to-width aspect ratios.

EL Tuhami [7] affirmed that Active lateral pressure delays the formation of flexural and diagonal shear cracks in the beam and limits the widths of such cracks. It also improves the aggregate interlock and consequently increases the concrete contribution to the flexural and shear resistance. The active pressure increases also the lateral confinement and enhances the mechanism of concrete confinement. A large increase was obtained in the stiffness and load-carrying capacity of the strengthened beams when compared to the reference un-strengthened ones.

## 2. EXPERIMENTAL PROGRAM:

The current research program focuses on the behavior of strengthened concrete prisms. The technique used for strengthening was the steel jacket welded under external prestressing. In

This technique, four steel angles were placed along the original prism corners. Then, external prestressing forces were applied in the two directions perpendicular to the direction of the acting vertical loads. After that, steel batten plates were welded horizontally over the corner angles just removing the prestressing forces. The experimental program described hereafter comprised a total of thirteen (13) tests of concrete prisms.

The main parameters varied through the test series are as follows: -

1. External confinement force value.
2. Aspect ratio of the prism.
3. Concrete strength.

### 2.1 Specimens Details:

As described in Table 1. Prisms were divided into four groups A, B, C, and D according to their concrete strength. Specimens in the same group were tested under different values of external confining pressure.

### 2.2 Material Properties

The material used throughout this program includes fine aggregate, coarse aggregate, cement, water, steel reinforcement and steel jacket used in applying torque.

#### 2.2.1 Fine Aggregate (Sand)

The used sand was clean from impurities, silt, loam and clay which are free from organic materials. Table 2 shows the main properties of sand.

#### 2.2.2 Coarse Aggregate

Crushed brown hard dolomite with a maximum size of 1/2" inch was used in this investigation. Table 3 shows the characteristics of the dolomite.

#### 2.2.3 Cement and Water

Ordinary Portland cement along with clean drinking water were used in all mixes in this research.

#### 2.2.4 Steel Cage

Steel cage consists of four angles with dimensions of 40 x 40 x 4 mm welded with horizontal batten plates with dimensions of 50 x 5 mm. Steel cage properties were tested in the National Center for Building Research as presented in Table 4.

**Table 1:** Details of the tested specimens.

| Group | Sample No | Sample Dimensions mm | Concrete $F_{cu}$ N/mm$^2$ | Angle Dimensions mm | Steel Strength Fy N/mm$^2$ | External Confining Torque N.m |
|---|---|---|---|---|---|---|
| A | 1 | 150 x 150 x 450 | 20 | NA | 370 | NA |
| | 2 | | | 40 x 40 x 4 | | 100 |
| | 3 | | | | | 150 |
| | 4 | | | | | 180 |
| B | 5 | 150 x 150 x 450 | 45 | NA | 370 | NA |
| | 6 | | | 40 x 40 x 4 | | 50 |
| | 7 | | | | | 100 |
| C | 8 | 150 x 150 x 450 | 50 | NA | 370 | NA |
| | 9 | | | 40 x 40 x 4 | | 50 |
| | 10 | | | | | 100 |
| | 11 | | | | | 150 |
| D | 12 | 150 x 300 x 450 | 40 | NA | 370 | NA |
| | 13 | | | 40 x 40 x 4 | | 50 |

**Table 2:** Properties of sand.

| Property | Test results |
|---|---|
| Specific gravity | 2.68 |
| Volume weight t/m$^3$ | 1.73 |

**Table 3:** Properties of Dolomite.

| Property | Test results |
|---|---|
| Specific gravity | 2.55 |
| Volume weight t/m$^3$ | 1.52 |

**Table 4:** Properties of steel cage.

| Type | Dimension mm | $F_y$ (MPa) | $F_u$ (MPa) |
|---|---|---|---|
| Steel Batten Plate | 50 x 5 | 298.7 | 438.5 |
| Steel Angle | 40 ×40 ×4 | 299.5 | 434.3 |

### 2.3 Mixes Concrete Design

The target concrete compressive strength in the current research was 20, 40, 45, and 50 MPa. Table 5 describes the mix properties of cubic meter for the required concrete compressive strength.

**Table 5:** Proportions of concrete mixes.

| Mix | Cement (kg/m³) | Sand (kg/m³) | Dolomite (kg/m³) | Water (kg/m³) | Super Plasticizer (% of cement weight) |
|---|---|---|---|---|---|
| **M 20** | 270 | 600 | 1000 | 189 | ---------- |
| **M 40** | 500 | 600 | 1000 | 215 | ---------- |
| **M 45** | 500 | 600 | 1000 | 180 | 3 % ASTM Type G Adecrite BVF |
| **M 50** | 500 | 600 | 1000 | 150 | 4 % ASTM Type G Adecrite BVF |

## 3. CASTING AND CURING

### 3.1 Molds

The molds employed for casting the prisms were fabricated from plywood sheets possessing a thickness of 25 mm and exhibiting exceptionally smooth surfaces. These molds were meticulously constructed to correspond with the precise dimensions of the tested prisms. In addition to the prisms, twelve cubes, each measuring 15 cm in length, were cast to ascertain the compressive strength of the concrete utilized in the prism specimens. Standard steel molds were employed for the casting of these cube specimens.

### 3.2 Casting and curing

Before casting, the prism molds were tightly assembled and checked for dimensional accuracy. The molds were cleaned well with an air jet and well-greased. Concrete mixed with proportions mentioned in the previous section was used to cast the specimens in the vertical direction.

## 4. STRENGTHENING PRISMS BEFORE TESTING

Twenty-eight days after the demolding process, the prisms were deemed ready for the strengthening procedure. The strengthening process commenced with the strategic placement of four steel angles, measuring 40 mm x 40 mm x 4 mm, at the corners of each prism. The length of these angles was carefully selected to be 44 cm, ensuring a dimension shorter than the prism's height. Following the placement of the steel angles, pressure casing comprising a steel form, and reinforcing rods were applied. These rods were subsequently tensioned using a torque key to achieve the desired confining pressure, as illustrated in Figure 1. Upon attaining the requisite prestressing pressure, batten plates, measuring 50 mm x 5 mm were welded to the corner steel angles, and subsequently, the pressure casing was removed. Additional batten plates were incorporated at the top and bottom of the prisms.

## 5. TEST SET-UP AND INSTRUMENTATION

A load cell was used to monitor, and record applied axial loads. The corresponding relative displacements were measured by 100 mm Linear Voltage Differential Transducers (LVDTs) as shown in Figure 2. Firstly, the prisms started to be loaded, and when the machine jack displacement reached the saved step in the computer which was measured by (LVDT) attached to the machine jack, the operator of the machine closed the valves of the hydraulic oil, then, the machine stopped loading the prism and computer software began to record the readings of the (LVDT). After finishing recording all data the machine operator opened the hydraulic oil valves and then the machine continued loading the prism until the jack base displacement reached the next step saved in the computer. The tests were terminated when the load suddenly dropped to a low fraction of the maximum load reading, resulting in a complete failure of the specimen.

**Figure 1:** Applying external pressure.

**Figure 2:** Test Setup.

## 6. EXPERIMENTAL TEST RESULTS

The twelve standard cubes were tested to determine the compressive strength of the concrete and compared with the design values as indicated in Table 6. Test results including the records of ultimate load capacity and vertical displacement values for the original prisms and the strengthened prisms as summarized in Table 7.

**Table 6:** Compressive strength of standard tested cubes

| Cube number | Tested concrete Strength ($Kg/cm^2$) | Average Concrete Strength ($Kg/cm^2$) | Designed concrete Strength ($N/mm^2$) |
|---|---|---|---|
| CU1 | 198 | 195.6 | 20 |
| CU2 | 207 | | |
| CU3 | 182 | | |
| CU4 | 462 | 449.3 | 45 |
| CU5 | 438 | | |
| CU6 | 448 | | |
| CU7 | 491 | 499.3 | 50 |
| CU8 | 518 | | |
| CU9 | 489 | | |
| CU10 | 412 | 411 | 40 |
| CU11 | 428 | | |
| CU12 | 393 | | |

**Table 7:** Experimental test results.

| Group | Sample No | Sample Dimensions mm | Concrete $F_{cu}$ $N / mm^2$ | External Confining TorqueN.m | $P_u$ kN | $P_u/P_u$ Control |
|---|---|---|---|---|---|---|
| A | 1 | 150 x 150 x 450 | 20 | NA | 303.76 | 100% |
| | 2 | | | 100 | 599.41 | 200% |
| | 3 | | | 150 | 729.3 | 243% |
| | 4 | | | 180 | 785.96 | 263% |
| B | 5 | 150 x 150 x 450 | 45 | NA | 441.56 | 100% |
| | 6 | | | 50 | 857.75 | 195% |
| | 7 | | | 100 | 934.28 | 214% |
| C | 8 | 150 x 150 x 450 | 50 | NA | 671.5 | 100% |
| | 9 | | | 50 | 922 | 137% |
| | 10 | | | 100 | 1096.3 | 164% |
| | 11 | | | 150 | 1222 | 182% |
| D | 12 | 150 x 300 x 450 | 40 | NA | 1227.28 | 100% |
| | 13 | | | 50 | 1695.72 | 140% |

Figures 3 to 6 describe the relationship between vertical load and corresponding vertical displacement for all tested groups. Figure 3 shows the comparison between the control specimen without strengthening and the prisms with strengthening in group A ($F_{cu}$ = 20 MPa). The figure illustrates that the influence of external confining pressure increases the ultimate load capacity by approximately 100% to 163%. Figure 4 shows the comparison between specimens in group B ($F_{cu}$ = 45 MPa), it illustrates that the influence of external confining pressure increases the ultimate load capacity of strengthened prisms comparing with the control prism without strengthening by approximately 95% to 114%.

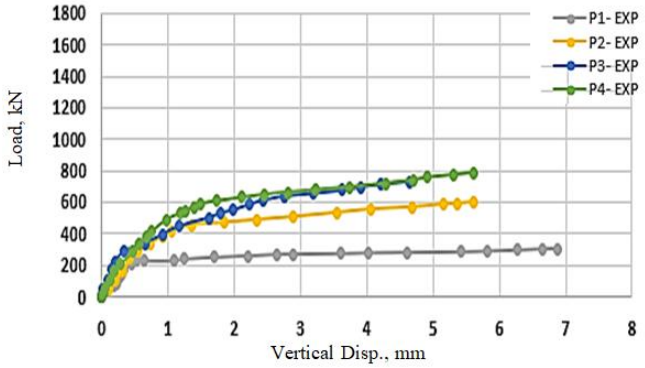


**Figure 3:** Vertical load versus Vertical displacement of group (A).

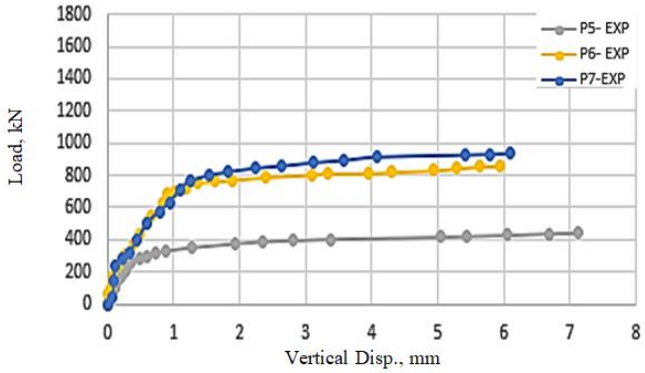


**Figure 4:** Vertical load versus Vertical displacement of group (B).

Figure 5 shows the comparison between the control specimen without strengthening and the prisms with strengthening in group C ($F_{cu}$ = 50 MPa). It shows that the impact of external confining pressure increases the ultimate load capacity by approximately 37% to 82%. Figure 6 shows the comparison between specimens in group D ($F_{cu}$ = 40 MPa) which has a rectangular section of 150 x 300 mm. It illustrates that the influence of external confining pressure raises the ultimate load capacity of strengthened prism compared with the control prism without strengthening by approximately 40%.

Finally, applying an external confining pressure on the concrete prisms increases the ultimate failure load, especially in case of weak concrete strength as in group (A).

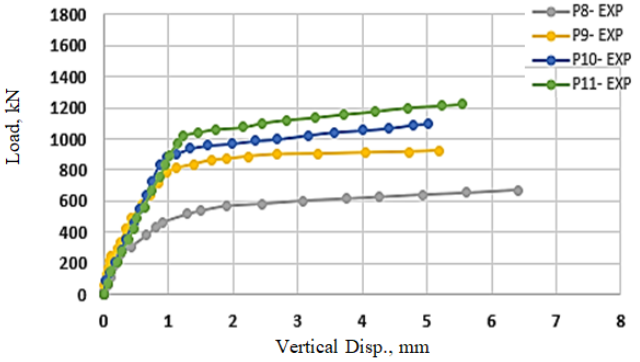


**Figure 5:** Vertical load versus Vertical displacement of group (C).

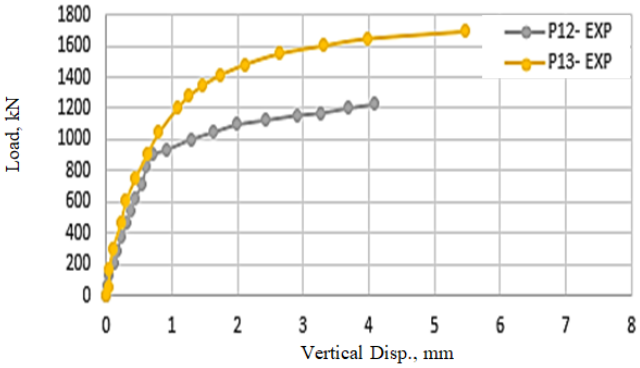


**Figure 6:** Vertical load versus Vertical displacement of group (D).

## 7. FINITE ELEMENT MODELING

The finite-element method, a common numerical approach, is widely used by researchers to evaluate the results of experimental studies. Three-dimensional finite-element (3DFE) analysis was developed as a powerful tool able to capture the concrete prisms' response. The commercial software ABAQUS 2021, which is based on the entry of the geometric and mechanical properties of the used materials, was used to create and analyze the 3D FE models provided throughout this research.

### 7.1 Elements Description and Mesh Size

#### 7.1.1 Solid (Brick) Element

Prisms were modeled using brick elements (C3D8R) as shown in Figure 7, Each node of this element has three transitional degrees of freedom. This element was chosen as it can define the boundaries of concrete prism property and can define the contact faces that are needed to apply load. Also, solid elements were used to model steel angles and batten plates which confined concrete prisms.

**Figure 7:** Solid element.

#### 7.1.2 Mesh Size

To reach the most accurate and close to the results of the experimental work, three models were generated for the control specimen with three different mesh sizes (5 mm, 10 mm, 15 mm). The models had the same material properties, element type, and load application. The most accurate results were generated from the model with 5 mm of mesh size as shown in Figure 8.

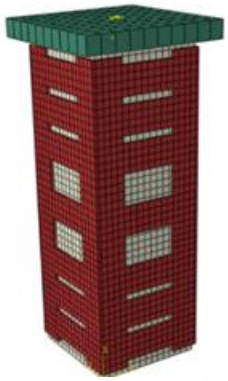

**Figure 8:** Mesh configuration of FE model.

### 7.2 Material Modeling

To model the concrete prisms, two different material models from ABAQUS [8] were used. These models include the concrete-damaged plasticity model (CDP) and the elastic-plastic model.

#### 7.2.1 Concrete Damaged Plasticity Model

The concrete damaged plasticity model available in ABAQUS was used to model concrete due to the ability of this model to simulate concrete's plastic properties and consider the behavior of concrete softening in tension and compression [9] as shown in Figure 9. Table 7 presents the concrete elastic properties while Table 9 shows concrete damaged plasticity model parameters used in the analysis.

#### 7.2.2 Elastic-Plastic Model

The elastic-plastic material model in ABAQUS was used to represent the behavior of steel angles and steel plates. Table 10 lists mechanical properties values used in finite element modeling to represent steel material.

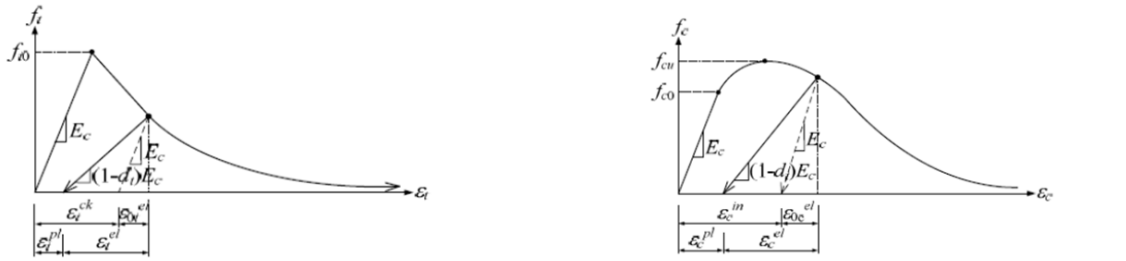

(**a**) Tensile behavior associated with tension stiffening. (**b**) Compression behavior associated with compression hardening.

**Figure 9:** Concrete damaged plasticity model [9].

**Table 8:** Elastic properties of concrete.

| Parameter | Concrete 20 MPa | Concrete 40 MPa | Concrete 45 MPa | Concrete 50 MPa |
|---|---|---|---|---|
| **Density, kg/m$^3$** | 2200 | 2200 | 2200 | 2200 |
| **Modulus of elasticity (Ec), MPa** | 20164 | 27828.04 | 29516.1 | 29368 |
| **Poisson's ratio (υ)** | 0.18 | 0.18 | 0.19 | 0.2 |

**Table 9:** Concrete damaged plasticity parameters [8].

| Parameter | Concrete 20 MPa | Concrete 40 MPa | Concrete 45 MPa | Concrete 50 MPa |
|---|---|---|---|---|
| **Dilation angle** | 37 | 40 | 41 | 41 |
| **Eccentricity** | 0.12 | 0.12 | 0.12 | 0.12 |
| **$f_{b0}/f_{c0}$** | 1.36 | 1.36 | 1.36 | 1.36 |
| **K** | 0.67 | 0.67 | 0.67 | 0.67 |
| **Viscosity parameter** | 0.00001 | 0.00001 | 0.00001 | 0.00001 |
| **Ultimate compressive stress** | 20 MPa | 40.34 MPa | 45.33 MPa | 50.1 MPa |
| **Ultimate tensile stress** | 2.1 MPa | 4.21 MPa | 4.63 MPa | 5.18 MPa |

**Table 10:** Mechanical properties of steel

| Parameter | Steel Plates and Angles |
|---|---|
| **Density, kg/m3** | 7860 |
| **Modulus of elasticity (Es), MPa** | 200000 |
| **Poisson's ratio (υ)** | 0.3 |
| **Yield strength, MPa** | 300 |
| **Ultimate strength, MPa** | 435 |

### 7.3 Boundary Conditions

In the Abaqus model tree, boundary conditions can be added using the load option and choosing to create boundary conditions. As shown in Figure 10, The bottom of the FE models was prevented from translation in all directions to simulate the experimental models which were supported from the bottom.

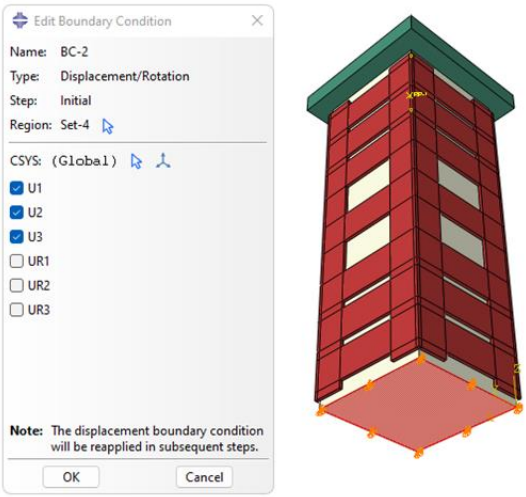


**Figure 10:** Boundary condition of FE model.

### 7.4 Loading

External confining pressure was simulated as a horizontal pressure acting on steel angles in both directions as a predefined field. Vertical load applied in steel plate over the prism head and increased till failure as shown in Figure 11.

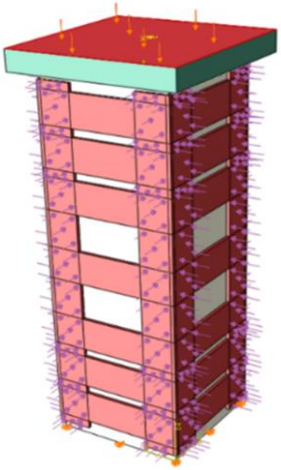

**Figure 11:** Loading of FE model.

## 8. FINITE ELEMENT RESULTS

Figure 12 presents the comparison between the control specimen without strengthening and the prisms with strengthening in group A ($F_{cu}$ = 20 MPa). The figure illustrates that the influence of external confining pressure increases the ultimate load capacity by approximately 150%.

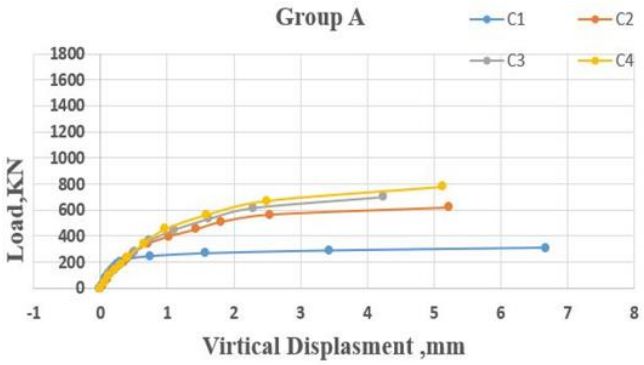


**Figure 12:** Vertical load versus Vertical displacement of group (A).

Figure 13 highlights the comparison between specimens in group B ($F_{cu}$ = 45 MPa), it illustrates that the influence of external confining pressure increases the ultimate load capacity of strengthened prisms compared with the control prism without strengthening by approximately 112%.

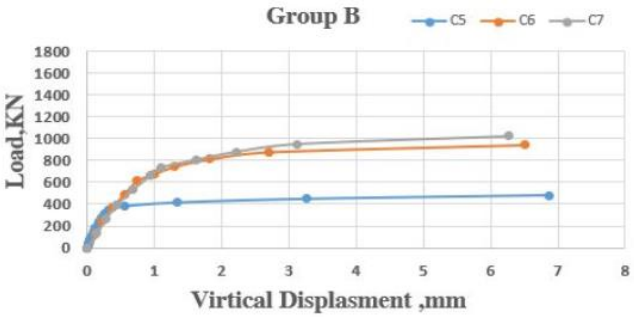


**Figure 13:** Vertical load versus Vertical displacement of group (B).

Figure 14 indicates the comparison between the control specimen without strengthening and the prisms with strengthening in group C ($F_{cu}$ = 50 MPa). It shows that the influence of external confining pressure increases the ultimate load capacity by approximately 106%.

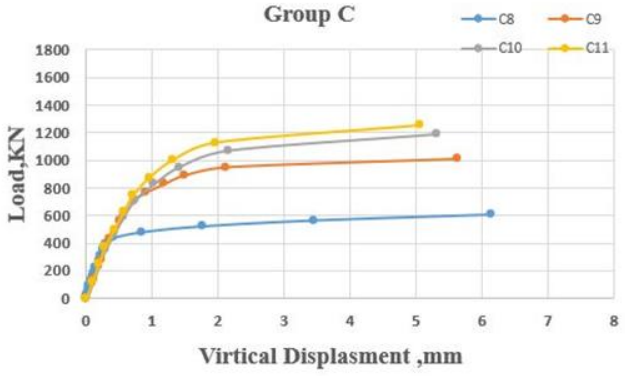


**Figure 14:** Vertical load versus Vertical displacement of group (C).

Figure 15 identifies the comparison between specimens in group D ($F_{cu}$ = 40 MPa) which has a rectangular section of 150 x 300 mm. It illustrates that the influence of external confining pressure increases the ultimate load capacity of strengthened prism compared with the control prism without strengthening by approximately 50%.

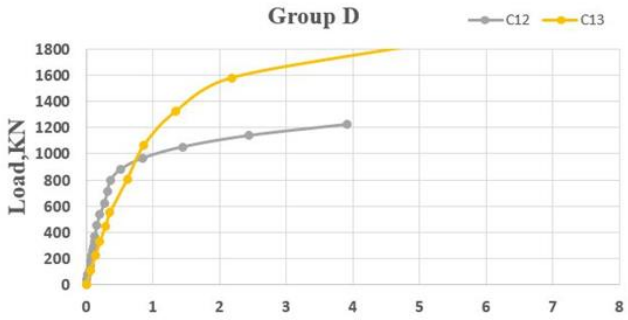


**Figure 15:** Vertical load versus Vertical displacement of group (D).

## 9. COMPARISON BETWEEN EXPERIMENTAL AND FE RESULTS

Experimental and finite element results of prism load capacity for thirteen models were summarized in Table 11. There is a high accuracy between experimental and FE results with a variation of 10 %.

Figures 16 to 28 displayed the relationship between axial load and corresponding vertical displacement for both experimental and F.E prisms models.

Figure 16 to 28 provides a clear view that the relationship between load versus displacement in experimental and finite elements modeling is the same. Therefore, the generated model can be used to study other relevant factors.

**Table 11:** Comparison between experimental and FE results.

| Model | EXP. | | FEM. | | Accuracy $P_{u\ FEM}/ P_{u\ EXP}$ |
|---|---|---|---|---|---|
| | V.Disp, mm | $P_u$, kN | V.Disp, mm | $P_u$, kN | |
| **P1** | 6.875 | 303.76 | 6.67 | 310.9 | **1.02** |
| **P2** | 5.62 | 599.41 | 5.22 | 632.345 | **1.06** |
| **P3** | 4.64 | 729.3 | 4.23 | 702.368 | **0.96** |
| **P4** | 5.61165 | 785.96 | 5.14 | 780.124 | **0.99** |
| **P5** | 7.13 | 441.56 | 6.87 | 480.97 | **1.09** |
| **P6** | 5.95 | 857.75 | 6.5 | 941.48 | **1.09** |
| **P7** | 6.1 | 934.28 | 6.26 | 1020.75 | **1.09** |
| **P8** | 6.4 | 671.5 | 6.14 | 607.65 | **0.9** |
| **P9** | 5.2 | 922 | 5.63 | 1010.256 | **1.1** |
| **P10** | 5.03 | 1096.3 | 5.31 | 1188.212 | **1.08** |
| **P11** | 5.54 | 1222 | 5.07 | 1255.368 | **1.03** |
| **P12** | 4.08 | 1227.28 | 3.91 | 1222.55 | **0.99** |
| **P13** | 5.463 | 1695.72 | 5.02423 | 1834.8795 | **1.08** |

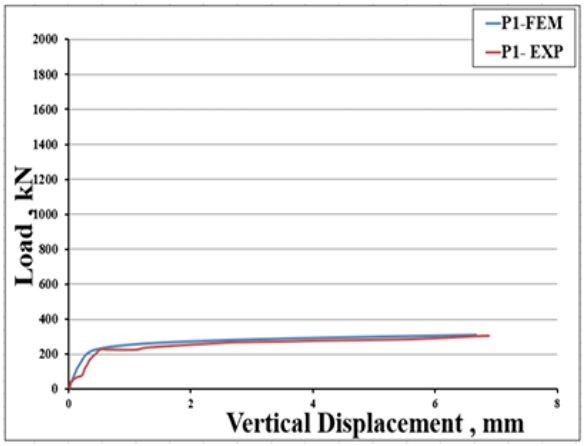


**Figure 16:** Load–displacement curve of P1.

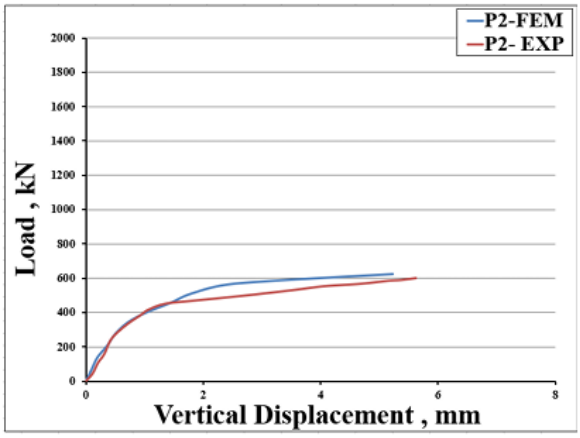


**Figure 17:** Load–displacement curve of P2.

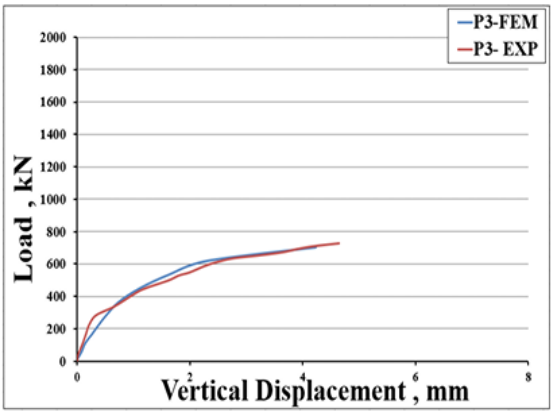


**Figure 18:** Load–displacement curve of P3.

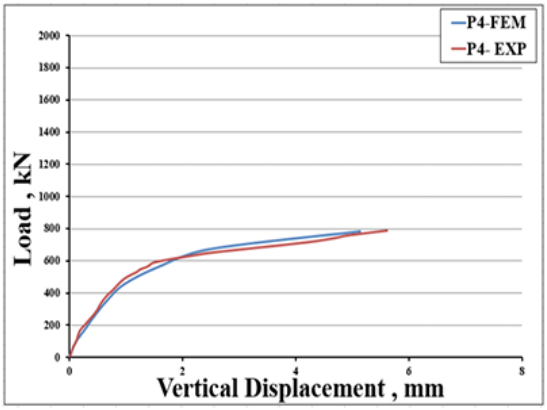


**Figure 19:** Load–displacement curve of P4.

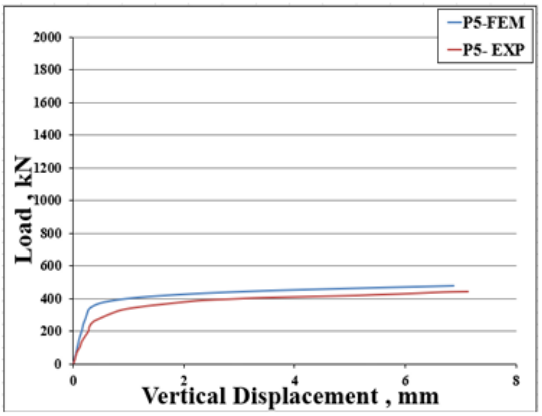


**Figure 20:** Load–displacement curve of P5.

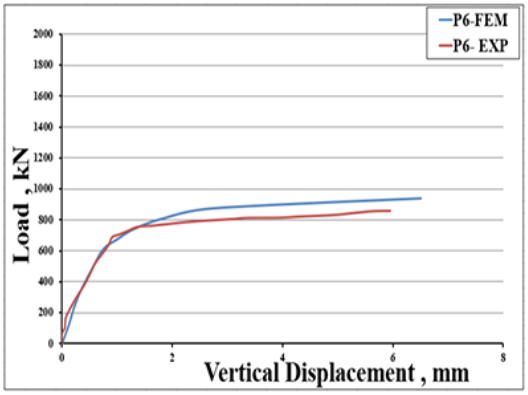


**Figure 21:** Load–displacement curve of P6.

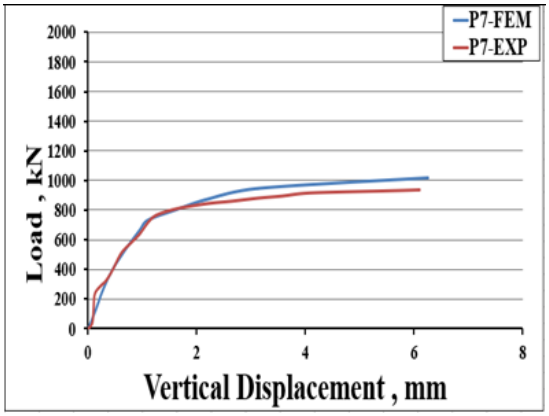


**Figure 22:** Load–displacement curve of P7.

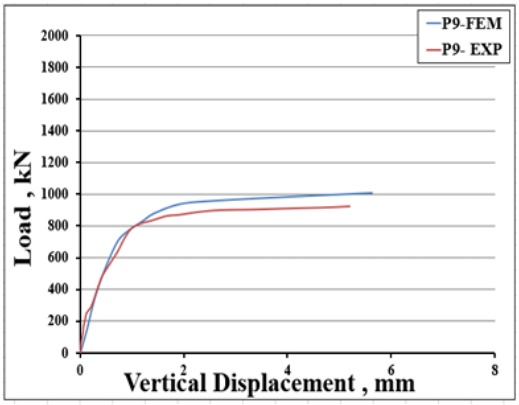


**Figure 23:** Load–displacement curve of P8.

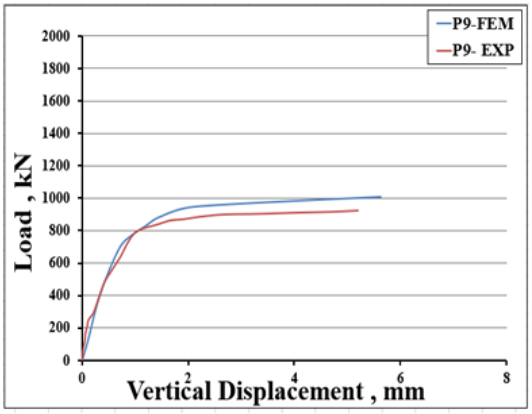


**Figure 24:** Load–displacement curve of P9.

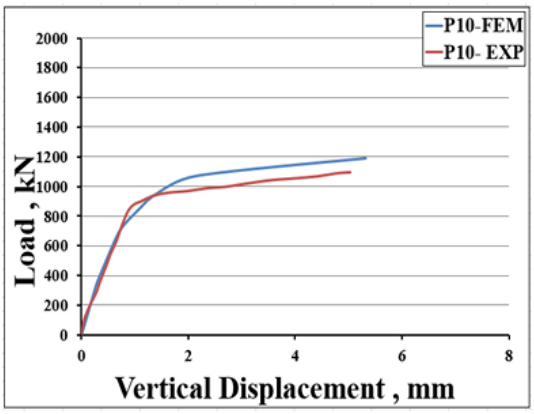


**Figure 25:** Load–displacement curve of P10.

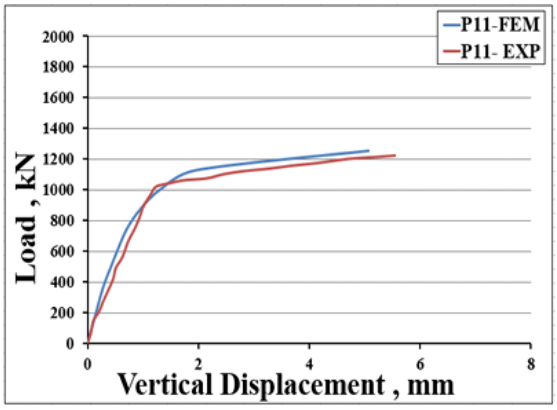


**Figure 26:** Load–displacement curve of P11.

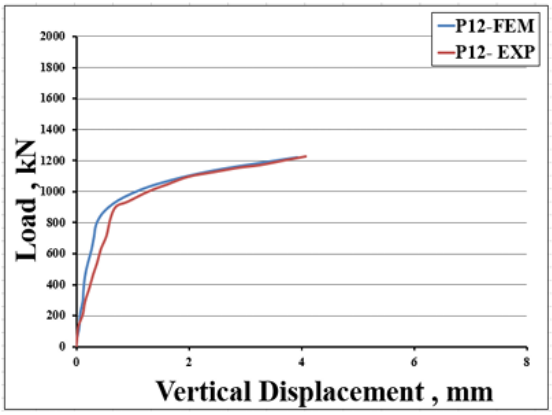


**Figure 27:** Load–displacement curve of P12.

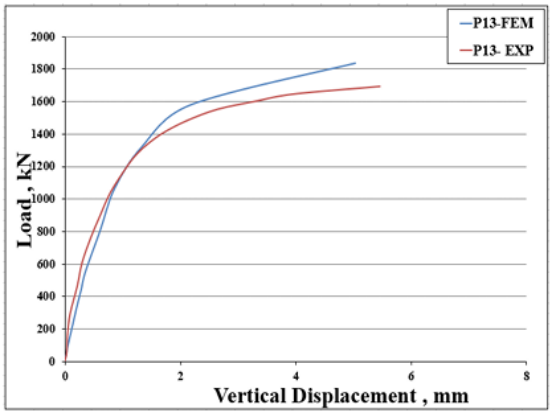


**Figure 28:** Load–displacement curve of P13.

### 9.1 Failure Pattern (creak pattern)

Figures 29 to 32 represent a comparison between failure modes and crack patterns of prism samples as detected and the corresponding FE failure mode, in which the same modes of failure happened.

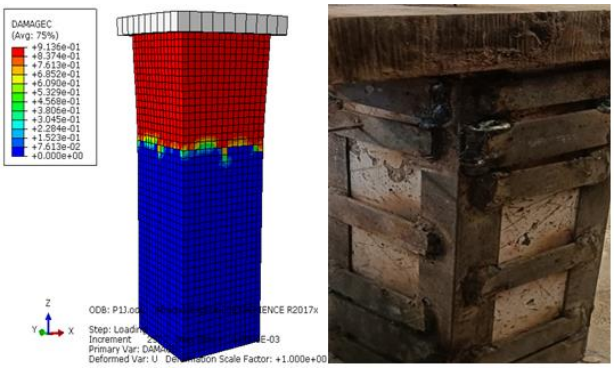

**(a)** FE Modeling. **(b)** Experimental.

**Figure 29:** Comparison between the crack pattern of the experimental model and its corresponding FE model of P2.

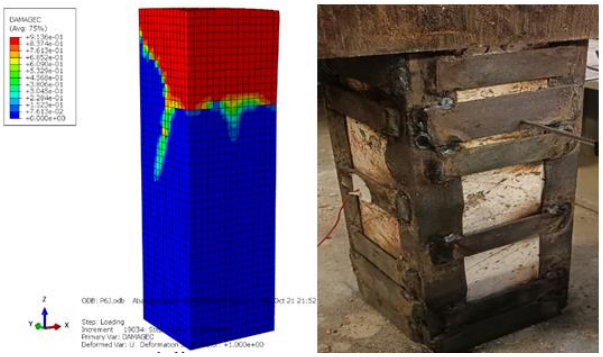

**(a)** FE Modeling. **(b)** Experimental.

**Figure 30:** Comparison between the crack pattern of the experimental model and its corresponding FE model of P6.

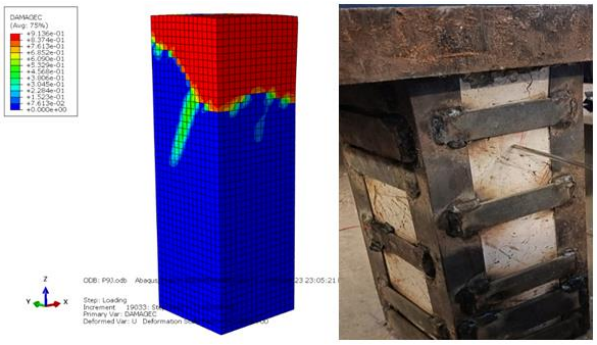

**(a)** FE Modeling. **(b)** Experimental.

**Figure 31:** Comparison between the crack pattern of the experimental model and its corresponding FE model of P9.

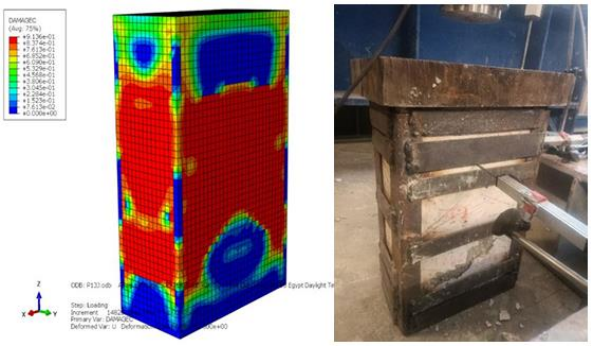

**(a)** FE Modeling. **(b)** Experimental.

**Figure 32:** Comparison between the crack pattern of the experimental model and its corresponding FE model of P13.

## 10. GOVERNING EQUATIONS AND DESIGN PROCEDURE

The following procedure is based on some empirical equations and simple relations known for steel and concrete section resistance. The procedure begins with the fact that the prism before strengthening has a specific ultimate load capacity calculated as:

**Pu = factor * δC*AC + factor * δs*As**

Where: -

Pu: ultimate prism load capacity.
δC : concrete compressive strength.
Ac: prism section area.
δs : steel strength.
As = steel section area.

The term of internal steel equals zero because there is no internal steel in prism samples.

Also, it can be assumed that the external confining pressure converted to concrete strength improves prism load capacity.

**Pt = (0.75*δC*AC +AC)** **(1)**

Where:-

Pt = target ultimate load of strengthened prism
δL = required applied lateral confining pressure
Ac = prism section area
δC = concrete compressive strength
X = constant factor.

Equation 1 was solved for the required lateral pressure δL which is to be applied to the prism by the proposed procedure. This pressure is attained by applying torque on the threaded rods surrounding the prism resulting in tension in the rod. To calculate the required lateral pressure δL the following equations can be used.

**Mt = 0.2*Tr*db** **(2)**

Where,

Mt = torque applied on threaded rods
Tr = tension on the threaded rods
db = rod diameter

Table 12 shows the results of substitution in Eq 2.

**Table 12:** Substitution in Equation 2.

| $M_t$ N.m | $M_t$ N.mm | $T_r$ N | $d_b$ mm |
|---|---|---|---|
| 50 | 50000 | 12500 | 20 |
| 100 | 100000 | 25000 | 20 |
| 150 | 150000 | 37500 | 20 |
| 180 | 180000 | 45000 | 20 |

**Tr = δL * L/2 * dp** **(3)**

Where,
Tr = tension on threaded rods
L = prism length
db = largest distance between threaded rods
δL= lateral pressure generated at the bottom of the corners
Table 13 shows the results of substitution in Eq 3.

**Table 13:** Substitution in Equation 3.

| Tr N | L/2 mm | dp mm | δL N/mm2 |
|---|---|---|---|
| 12500 | 75 | 200 | 0.833 |
| 25000 | 75 | 200 | 1.666 |
| 37500 | 75 | 200 | 2.5 |
| 45000 | 75 | 200 | 3 |

To calculate the required constant factor (X) the following equations can be used.

For ordinary concrete strength

**X= 25* M* L/b * (Lh/Lv)** **(4)**

For high-strength concrete

**X= 10* L/b *( Lh/Lv)**

Where,

M = reduction factor
(M=1 in case of internal steel reinforcement, M= 0.6 in case of without internal steel reinforcement)
Lv = distance between center line of horizontal plate and the top of next plate
L = prism length
Lh = width of the horizontal plate
b = prism width

Table 14 shows the results of substitution in Eq 4.
Table 15 shows the results of substitution in Eq 1. It clearly shows that there is a high accuracy between the experimental results and equation results with a variation of 10 %.

## 11. CONCLUSION

The present study showed that strengthening using a steel jacket welded under surrounding external pressure can be successfully used for increasing the ultimate baring capacity of concrete prisms. The following summarizes the conclusions of this investigation:

1- Prisms with ordinary concrete strength (Fcu=20 N/mm$^2$), the ultimate load capacity of the strengthened prisms increased up to 263%.
2- Prisms with high-strength concrete (Fcu=40:50 N/mm$^2$), the ultimate load capacity of the strengthened prisms increased up to 214%.
3- It was found that, there was a great effect of applying external confining pressure on ordinary concrete compared to high-strength concrete.
4- It can clearly be observed that applying external confining pressure has a greater effect in the case of square prism section with respect to rectangular section.
5- At a certain stage, increasing external confining pressure leads to slight effect on increasing ultimate load capacity of prisms.
6- There was a good agreement between experimental and finite element results within ±10% difference percentage.
7- The equations proposed in this study can be used to calculate the prism capacity after strengthening, as it showed a good prediction with the experimental results within ±10% difference percentage.

**Table 14:** Substitution in Equation 4.

| Prism | Concrete | L/b | M | $L_h/L_v$ | X |
|---|---|---|---|---|---|
| P1 | Ordinary | | | | |
| P2 | | 1 | 0.6 | 0.471 | 7.1 |
| P3 | | 1 | 0.6 | 0.471 | 7.1 |
| P4 | | 1 | 0.6 | 0.471 | 7.1 |
| P5 | High-Strength | | | | |
| P6 | | 1 | 1 | 0.471 | 4.7 |
| P7 | | 1 | 1 | 0.471 | 4.7 |
| P8 | | | | | |
| P9 | | 1 | 1 | 0.471 | 4.7 |
| P10 | | 1 | 1 | 0.471 | 4.7 |
| P11 | | 1 | 1 | 0.471 | 4.7 |
| P12 | | | | | |
| P13 | | 2 | 1 | 0.471 | 9.4 |

**Table 15:** Substitution in Equation 1.

| Prism | $\delta_C$ $N/mm^2$ | $\delta_L$ $N/mm^2$ | X | $A_C$ $mm^2$ | $P_t$ from Equation (kN) | $P_t$ from tests (kN) | Percentage of Equation Validity |
|---|---|---|---|---|---|---|---|
| P1 | | | | | | | |
| P2 | 20 | 1.67 | 7.1 | 22500 | 603.644 | 600 | 99 % |
| P3 | 20 | 2.5 | 7.1 | 22500 | 736.875 | 730 | 99 % |
| P4 | 20 | 3 | 7.1 | 22500 | 816.750 | 790 | 97 % |
| P5 | | | | | | | |
| P6 | 45 | 0.833 | 4.7 | 22500 | 847.465 | 860 | 99 % |
| P7 | 45 | 1.67 | 4.7 | 22500 | 935.555 | 940 | 100 % |
| P8 | | | | | | | |
| P9 | 50 | 0.833 | 4.7 | 22500 | 931.840 | 920 | 101 % |
| P10 | 50 | 1.67 | 4.7 | 22500 | 1019.930 | 1100 | 93 % |
| P11 | 50 | 2.5 | 4.7 | 22500 | 1108.125 | 1220 | 110 % |
| P12 | | | | | | | |
| P13 | 40 | 0.833 | 9.4 | 45000 | 1702.359 | 1700 | 100% |

## REFERENCES


[1] Priestley M. J., Seible F., Xiao Y. and Verma R. "Steel Jacket Retrofitting of Reinforced Concrete Bridge Columns for Enhanced Shear Strength-Part 1: Theoretical Consideration and Test Design", ACI, Struct. J., Vol.91, No. 4, pp.394-405, July-Aug, 1994.

[2] Lisantono, Ade, Agung Budiman, and Paulinus Haesler Boantua Sidauruk. "Experimental investigation of reinforced concrete column embedded with the angle steel shapes." Procedia Engineering 125 (2015).

[3] Al-Tuhami, A.A. & Sakr, T.A., An Innovative Technique for Strengthening Reinforced Concrete Elements Using Mechanical External Prestressing. Proceeding of the Eighth Arab Structural Engineering Conference, Cairo, pp. 761-775, 2000

[4] A. A. Al-Tuhami & T. A. Sakr "Retrofit of reinforced concrete columns using global lateral external pressure" Composites in Constructions, Bruno et al (eds), 2003, Editoriale Bios

[5] Al-Tuhami AbuZeid. "Method and apparatus for strengthening the concrete elements using prestressing confinement." U.S. Patent No. 6,718,723. 13 Apr. 2004.

[6] AL-TUHAMI ABUZEID AL-TUHAMI "RETROFITTING OF RC COLUMNS WITH ACCESSIBLE AND INACCESSIBLE FACES USING THE MECHANICAL STRENGTHENING TECHNIQUE" The 10th Arab Structural Engineering Conference, 13-15 November 2006, Kuwait.

[7] A. A. AL-TUHAMI "RETROFITTING OF RC BEAMS USING ACTIVE EXTERNAL PRESSURE" AICSGE 6, Structural Engineering Dept., Faculty of Engineering, Alexandria University 15-17 April 2007.

[8] Abaqus Documentation User's Guide: ABAQUS User's Guide: Dassault Systemes, Simulia Corp, Providence, 2021.

[9] Hu, Hsuam-Teh, and William C. Schnobrich. "Constitutive Modeling of Concrete by Using Nonassociated Plasticity", Journal of Materials in Civil Engineering 1, no. 4, P.P:199-216, 1989.